

# Effect of intense magnetic fields on reduced-magnetohydrodynamics evolution in $\sqrt{s_{NN}} = 200$ GeV Au + Au collisions

Victor Roy,<sup>1</sup> Shi Pu,<sup>2</sup> Luciano Rezzolla,<sup>3,4</sup> and Dirk H. Rischke<sup>3,5</sup><sup>1</sup>*National Institute of Science Education and Research, HBNI, 752050 Odisha, India*<sup>2</sup>*Department of Physics, The University of Tokyo, 7-3-1 Hongo, Bunkyo-ku, Tokyo 113-0033, Japan*<sup>3</sup>*Institute for Theoretical Physics, Goethe University, Max-von-Laue-Str. 1, D-60438 Frankfurt am Main, Germany*<sup>4</sup>*Frankfurt Institute for Advanced Studies, Ruth-Moufang-Str. 1, D-60438 Frankfurt am Main, Germany*<sup>5</sup>*Department of Modern Physics, University of Science and Technology of China, Hefei, Anhui 230026, China*

(Received 19 June 2017; revised manuscript received 27 October 2017; published 30 November 2017)

We investigate the effect of large magnetic fields on the  $(2 + 1)$ -dimensional reduced-magnetohydrodynamical expansion of hot and dense nuclear matter produced in  $\sqrt{s_{NN}} = 200$  GeV Au+Au collisions. For the sake of simplicity, we consider the case where the magnetic field points in the direction perpendicular to the reaction plane. We also consider this field to be external, with energy density parametrized as a two-dimensional Gaussian. The width of the Gaussian along the directions orthogonal to the beam axis varies with the centrality of the collision. The dependence of the magnetic field on proper time ( $\tau$ ) for the case of zero electrical conductivity of the QGP is parametrized following Deng *et al.* [*Phys. Rev. C* **85**, 044907 (2012)], and for finite electrical conductivity following Tuchin [*Phys. Rev. C* **88**, 024911 (2013)]. We solve the equations of motion of ideal hydrodynamics for such an external magnetic field. For collisions with nonzero impact parameter we observe considerable changes in the evolution of the momentum eccentricities of the fireball when comparing the case when the magnetic field decays in a conducting QGP medium and when no magnetic field is present. The elliptic-flow coefficient  $v_2$  of  $\pi^-$  is shown to increase in the presence of an external magnetic field and the increment in  $v_2$  is found to depend on the evolution and the initial magnitude of the magnetic field.

DOI: [10.1103/PhysRevC.96.054909](https://doi.org/10.1103/PhysRevC.96.054909)

## I. INTRODUCTION

Two positively charged heavy nuclei produce ultraintense magnetic fields in collider experiments at the Relativistic Heavy Ion Collider (RHIC) and at the Large Hadron Collider (LHC), e.g.,  $B \sim 10^{18}$ – $10^{19}$  G for  $\sqrt{s_{NN}} = 200$  GeV Au+Au collisions. The intensity of the magnetic field in the transverse plane grows approximately linearly with the center-of-mass energy ( $\sqrt{s_{NN}}$ ) [1–3] (see also recent studies including nonzero chiral conductivity [4,5]). The corresponding electric field in the transverse plane also becomes very large since it is enhanced by a Lorentz factor. Such intense electric and magnetic fields are believed to have a strong impact on the dynamics of high-energy heavy-ion collisions. For example, a strong magnetic field may induce energy loss of fast quarks and charged leptons via synchrotron radiation [6], or may enhance dilepton and photon production [7,8]. There are several other interesting phenomena related to the presence of ultraintense magnetic fields in heavy-ion collisions. For example, in the case of an imbalance in the number of left- vs. right-handed fermions, a charge current is induced in the quark-gluon plasma (QGP), leading to the separation of electrical charges, which is known as the chiral magnetic effect (CME) [9]. Within a  $(3 + 1)$ -dimensional anomalous hydrodynamics calculation, Ref. [10] showed that the CME could be seen in azimuthal correlations of charged hadrons. Along with the CME, it was also theoretically predicted that massless fermions with the same charge but different chirality will be separated, known as chiral separation effect (CSE). A connection between these effects and the Berry phase in condensed-matter systems was pointed out in Refs. [11–16], and some nonlinear chiral

transport phenomena were studied in Refs. [17–20]. Within the statistical hadron-resonance gas model of Ref. [21], significant changes of hadron multiplicities were observed in the presence of a strong magnetic field. Finally, the possibility of a change in the quark-hadron phase transition line in the QCD phase diagram under the combined influence of external magnetic field and local vortices was explored in Ref. [22]; we refer the reader to the recent reviews [23–27], where more details can be found.

Relativistic dissipative hydrodynamics has so far been successfully applied to explain the experimentally measured flow harmonics in heavy-ion collisions. The success of hydrodynamics implies that a QGP with small shear-viscosity to entropy-density ratio is formed in Au+Au collisions at top RHIC energies within a short time interval  $\sim 0.2$ – $0.6$  fm [28–35]. The system is close to local equilibrium, thus the initial geometry of the collision has a strong influence on the final momentum anisotropy. However, the possible effect of a magnetic field on the hydrodynamical evolution has so far not been studied extensively, except for some simplified cases [36,37] and most recently using some approximate form of the equations of relativistic magnetohydrodynamics (MHD) [38,39], or employing a  $(3 + 1)$ -dimensional partonic cascade Boltzmann approach to multiparton scatterings (BAMPS) [40].

In a parallel analytical approach, in Refs. [41–43] solutions of the ideal-MHD equations were found in simplified geometries. More specifically, for Au+Au collisions at  $\sqrt{s_{NN}} = 200$  GeV, the electromagnetic field energy was shown to be comparable to the initial energy density of the QGP in Ref. [44]. In a recent work [45], it was argued that a magnetic

field of magnitude  $eB \sim m_\pi^2 \sim 10^{18} - 10^{19}$  G, with  $m_\pi$  the pion mass, can induce a large azimuthal anisotropy of the produced particles. In Refs. [46,47] it was also shown that the magnitude of the shear viscosity extracted from the experimental data is underestimated when ignoring the magnetic field. On the other hand, Ref. [38] has found that the elliptic flow is reduced in the presence of a magnetic field when one considers a temperature-dependent magnetic susceptibility of the QGP. Similarly, in Ref. [48] magnetic fields were found to have only a very small impact on the flow harmonics within the parton hadron string model.

Here we will study the  $(2+1)$ -dimensional expansion of matter with vanishing magnetization in terms of the dynamics of a perfect fluid [49] in the presence of an external magnetic field. We refer to this approach as reduced MHD and we note that this is not a self-consistent solution of the full set of MHD equations, since we only use a parametrized form for the evolution of the magnetic field and do not solve Maxwell's equations together with the conservation equations of energy and momentum. For the sake of simplicity, we also assume that the electrical conductivity is infinite (i.e., the ideal-MHD limit), since this allows us to eliminate the electric field in favor of the magnetic field (see below). Contrasting our approach with the one of Ref. [50], it is useful to remark that they are quite complementary. In fact, while in Ref. [50] the full set of ideal-MHD equations was employed, it was solved only for a comparatively small value of the initial magnetic field and for a simple ultrarelativistic equation of state (EOS). Here instead, we employ the reduced-MHD formulation, but study the impact of varying the initial magnetic field strength, adopting, furthermore, a realistic EOS.

We should also note that, in principle, one should then not use a parametrized form for the magnetic-field evolution, because for a perfectly conducting fluid one can show that the magnetic field follows the evolution of the entropy density (the so-called frozen-flux theorem, see Refs. [41,42]). Vice versa, using some parametrized form of the magnetic field generally implies that the electric conductivity is finite. Assuming a perfectly conducting fluid under the influence of an external magnetic field still represents a reasonable first approximation, which, however, calls for a future improvement towards a self-consistent MHD solution, along the lines of the work carried out in Ref. [50]. We also assume that the magnetic field only points into the  $y$  direction. In Ref. [44] this was shown to be a good approximation for peripheral collisions. In a first approximation, we will also neglect the magnetization of the QGP and the change in the EOS due to the magnetic field. We then investigate the effect of the magnetic field on the fluid evolution and the momentum anisotropy of charged particles on an event-averaged basis. The goal of our study is to clarify how large the external magnetic field has to be and how slowly it has to decay in order to make a sizable impact on the momentum anisotropy of charged particles.

The paper is organized as follows: in Sec. II we discuss the mathematical formalism employed in our calculations, while the numerical setup is presented in Sec. III. Our results are discussed in detail in Sec. IV and a summary is given at the end in Sec. V. We use natural units  $\hbar = c = \epsilon_0 = \mu_0 = 1$ , where  $\epsilon_0$  and  $\mu_0$  are the electric permittivity and magnetic

permeability in vacuum, respectively, and the electric charge  $e := \sqrt{4\pi\hbar c\alpha} \simeq 0.303$ , where  $\alpha \simeq 1/137$  is the fine-structure constant. In these units the quantity  $eB$  has dimension  $\text{GeV}^2$ . Throughout the paper the components of four-tensors are indicated with greek indices, whereas three-vectors are denoted as boldface symbols. The metric tensor in flat space time is  $g^{\mu\nu} = \text{diag}(+, -, -, -)$ .

## II. MAGNETOHYDRODYNAMICS

We consider a system consisting of matter, represented by a QGP with electric charge, and fields, i.e., electromagnetic fields, which are created in the collision of heavy ions. The space-time evolution of the coupled system of QGP and electromagnetic field is obtained by solving the equations of motion of MHD, i.e., energy-momentum conservation coupled to Maxwell's equations. In order to relate our work to that of others, we first discuss the MHD equations of nondissipative, polarized, and magnetized fluids in general [51–53], and then specialize to the case of a perfectly conducting, nondissipative fluid.

### A. MHD of nondissipative, polarized, and magnetized fluids

The energy-momentum conservation equation reads

$$\partial_\nu T^{\mu\nu} = 0, \quad (1)$$

with  $T^{\mu\nu}$  being the total energy-momentum tensor. The latter can be decomposed into a matter part,  $T_{\text{mat}}^{\mu\nu}$ , and a field part,  $T_{\text{field}}^{\mu\nu}$ , such that

$$T^{\mu\nu} = T_{\text{mat}}^{\mu\nu} + T_{\text{field}}^{\mu\nu}, \quad (2)$$

but this decomposition is not unique. Following Israel [52], for a nondissipative, polarized, and magnetized fluid we define (note that our convention for the metric tensor differs from that of Israel [52] by an overall sign)

$$T_{\text{mat}}^{\mu\nu} := (\varepsilon + p)u^\mu u^\nu - p g^{\mu\nu} - \Pi^\mu u^\nu, \quad (3)$$

$$T_{\text{field}}^{\mu\nu} := F^\mu{}_\alpha H^{\alpha\nu} + \frac{1}{4}g^{\mu\nu} F_{\alpha\beta} F^{\alpha\beta}, \quad (4)$$

where  $\varepsilon$  and  $p$  are energy density and pressure of the fluid, respectively, and  $u^\mu := \gamma(1, \mathbf{v})$  is the four-velocity of the fluid in an arbitrary frame [in our context we choose the center-of-momentum (CM) frame of the heavy-ion collision], where the fluid moves with three-velocity  $\mathbf{v}$ ;  $\gamma := (1 - v^2)^{-1/2}$  is the Lorentz factor.<sup>1</sup> Introducing antisymmetrization of a rank-two tensor  $A^{\mu\nu}$  via the notation  $A^{[\mu\nu]} := \frac{1}{2}(A^{\mu\nu} - A^{\nu\mu})$ , the auxiliary vector  $\Pi^\mu$  in Eq. (3) is defined as [52]

$$\Pi^\mu := 2u_\lambda F^{[\mu}{}_\nu M^{\lambda]\nu}, \quad (5)$$

where

$$F^{\mu\nu} = E^\mu u^\nu - E^\nu u^\mu + \epsilon^{\mu\nu\alpha\beta} u_\alpha B_\beta \quad (6)$$

is the Faraday tensor. Here,  $\epsilon^{\mu\nu\alpha\beta}$  is the completely antisymmetric four-tensor,  $\epsilon^{0123} = \sqrt{\det|g|}$  with  $g_{\mu\nu}$  being the

<sup>1</sup>Note that hereafter we will indicate spatial three-vectors with a bold face, i.e.,  $\mathbf{V} = \vec{\mathbf{V}}$ .

metric tensor,  $E^\mu := F^{\mu\nu}u_\nu$  is the electric field and  $B^\mu := \frac{1}{2}\epsilon^{\mu\nu\alpha\beta}u_\nu F_{\alpha\beta}$  the magnetic induction field, both measured in a frame comoving with the fluid. Note that by definition  $E^\mu$  and  $B^\mu$  are orthogonal to  $u^\mu$ , i.e.,  $E^\mu u_\mu = B^\mu u_\mu = 0$ . Also, both  $E^\mu$  and  $B^\mu$  are spacelike vectors, i.e.,  $0 > E^\mu E_\mu$  and  $0 > B^\mu B_\mu =: -B^2$ .

The in-medium Faraday tensor in Eq. (4) is defined as  $H^{\mu\nu} := F^{\mu\nu} - M^{\mu\nu}$ , where

$$M^{\mu\nu} = -P^\mu u^\nu + P^\nu u^\mu + \epsilon^{\mu\nu\alpha\beta}u_\alpha M_\beta \quad (7)$$

is the polarization tensor, also appearing in Eq. (5), with the polarization vector  $P^\mu := -M^{\mu\nu}u_\nu$  and the magnetization vector  $M^\mu := \frac{1}{2}\epsilon^{\mu\nu\alpha\beta}u_\nu M_{\alpha\beta}$ . Note that also  $P^\mu$  and  $M^\mu$  are orthogonal to  $u_\mu$ , i.e.,  $P^\mu u_\mu = M^\mu u_\mu = 0$ , as well as being spacelike, i.e.,  $0 > P^\mu P_\mu$ ,  $0 > M^\mu M_\mu$ . Hereafter, we will assume that  $P^\mu = \chi_E E^\mu$  and  $M^\mu = \chi_B B^\mu$ , which is characteristic for matter with a linear response to electromagnetic fields.

Inserting Eqs. (6) and (7) into Eq. (5) yields

$$\Pi^\mu = \epsilon^{\mu\nu\alpha\beta}u_\nu(M_\alpha E_\beta - P_\alpha B_\beta), \quad (8)$$

so that in the comoving frame

$$\Pi^0 = 0, \quad \text{and} \quad \mathbf{\Pi} = \mathbf{P} \times \mathbf{B} - \mathbf{M} \times \mathbf{E}. \quad (9)$$

Note that neither  $T_{\text{mat}}^{\mu\nu}$  nor  $T_{\text{field}}^{\mu\nu}$  are by themselves symmetric, but their sum is,  $T^{\mu\nu} = T^{\nu\mu}$ . To see this, compute their anti-symmetric parts  $T_{\text{mat}}^{[\mu\nu]} = -\Pi^{[\mu}u^{\nu]}$  and  $T_{\text{field}}^{[\mu\nu]} = -F^{[\mu}{}_\alpha H^{\nu]\alpha} \equiv F^{[\mu}{}_\alpha M^{\nu]\alpha}$  and use the identity (see Eq. (6.24) of Ref. [52])

$$\Pi^{[\mu}u^{\nu]} = F^{[\mu}{}_\alpha M^{\nu]\alpha}, \quad (10)$$

which can be readily proven using Eqs. (6) and (7), together with the assumption that the response of the matter to electromagnetic fields is linear.

A decomposition of the energy-momentum tensor where each term is symmetric by itself reads [52]

$$T^{\mu\nu} = T_{\text{sym}}^{\mu\nu} + T_{\text{free field}}^{\mu\nu}, \quad (11)$$

with the symmetric free energy-momentum tensor of the electromagnetic field

$$T_{\text{free field}}^{\mu\nu} := F^\mu{}_\alpha F^{\alpha\nu} + \frac{1}{4}g^{\mu\nu}F_{\alpha\beta}F^{\alpha\beta}, \quad (12)$$

and the symmetric matter energy-momentum tensor

$$\begin{aligned} T_{\text{sym}}^{\mu\nu} &:= T_{\text{mat}}^{\mu\nu} + F^\mu{}_\alpha M^{\nu\alpha} \\ &= (\varepsilon + p)u^\mu u^\nu - pg^{\mu\nu} - \Pi^{(\mu}u^{\nu)} + F^{(\mu}{}_\alpha M^{\nu)\alpha}, \end{aligned} \quad (13)$$

where we used Eq. (10) and introduced a symmetrized rank-two tensor via the notation  $A^{(\mu\nu)} := \frac{1}{2}(A^{\mu\nu} + A^{\nu\mu})$ .

Note that the definitions of energy-momentum tensor  $T_{\text{mat}}^{\mu\nu}$  in Refs. [42,55] do not contain the terms proportional to the auxiliary vector  $\Pi^\mu$ . This is because for the physical conditions encountered in relativistic heavy-ion collisions, both electromagnetic susceptibilities  $\chi_E$  and  $\chi_B$ , as well as the ratio of the electromagnetic energy density to fluid energy density are usually much smaller than unity [44], so that  $\Pi_\mu/(\varepsilon + p) \sim \chi_{E,B}B^2/(\varepsilon + p) \ll 1$ , and the auxiliary vector  $\Pi^\mu$  can be neglected as a first approximation.

Maxwell's equations in matter read

$$\partial_\mu H^{\mu\nu} = j^\nu, \quad \partial_\mu \tilde{F}^{\mu\nu} = 0, \quad (14)$$

where  $j^\nu := \rho u^\nu$  is the electric-charge four-current, with the net electric charge density  $\rho$ , and  $\tilde{F}^{\mu\nu} := \frac{1}{2}\epsilon^{\mu\nu\alpha\beta}F_{\alpha\beta}$  is the dual Faraday tensor. Using these equations, one can show that

$$\partial_\nu T_{\text{field}}^{\mu\nu} = -F^{\mu\nu}j_\nu + \frac{1}{2}M_{\alpha\beta}\partial^\mu F^{\alpha\beta}. \quad (15)$$

Moreover, using the Boltzmann equation, Israel [52] proved that

$$\partial_\nu T_{\text{mat}}^{\mu\nu} = F^{\mu\nu}j_\nu - \frac{1}{2}M_{\alpha\beta}\partial^\mu F^{\alpha\beta}, \quad (16)$$

so that the sum of both equations indeed gives total energy-momentum conservation, Eq. (1). This implies that the symmetric matter energy-momentum tensor obeys the equation

$$\partial_\nu T_{\text{sym}}^{\mu\nu} = F^{\mu\nu}(j_\nu + \partial_\lambda M^\lambda{}_\nu). \quad (17)$$

## B. Ideal MHD

The electric current induced by an electric field is  $j_{\text{ind}}^\mu := \sigma E^\mu$ , where  $\sigma$  is the electric conductivity. Since for a perfect conductor,  $\sigma \rightarrow \infty$ , we have to demand that  $E^\mu \rightarrow 0$ , otherwise the induced current would be infinite. This simplifies the equations of motion of MHD considerably, because in this case also  $P^\mu = \chi_E E^\mu \rightarrow 0$ , which eliminates the auxiliary vector  $\Pi^\mu$  in Eq. (5) from the discussion. The matter energy-momentum tensor becomes that of a nondissipative fluid in the absence of fields,

$$T_{\text{mat}}^{\mu\nu} \rightarrow (\varepsilon + p)u^\mu u^\nu - pg^{\mu\nu}, \quad (18)$$

while the symmetric matter energy-momentum tensor assumes the form given in Eq. (4) of Ref. [55],

$$T_{\text{sym}}^{\mu\nu} \rightarrow (\varepsilon + p)u^\mu u^\nu - pg^{\mu\nu} + F^{(\mu}{}_\alpha M^{\nu)\alpha}. \quad (19)$$

For a linear response of matter to the magnetic induction field,  $M^\mu = \chi_B B^\mu$ , the total energy-momentum tensor can then be brought into the form<sup>2</sup> [42,54–56]

$$\begin{aligned} T^{\mu\nu} &= (\varepsilon + p - MB + B^2)u^\mu u^\nu \\ &\quad - (p - MB + \frac{1}{2}B^2)g^{\mu\nu} + (MB - B^2)b^\mu b^\nu \\ &= [\varepsilon + p + B^2(1 - \chi_B)]u^\mu u^\nu \\ &\quad - [p + \frac{1}{2}B^2(1 - 2\chi_B)]g^{\mu\nu} + B^2(1 - \chi_B)b^\mu b^\nu, \end{aligned} \quad (20)$$

where  $M = \sqrt{-M^\mu M_\mu}$  and  $b^\mu = B^\mu/B$ . Note that because of  $E^\mu = 0$ , the electric field  $\vec{E}$  in the CM frame can be eliminated in favor of the magnetic induction field  $\vec{B}$  in the CM frame via  $\vec{E} = -\mathbf{v} \times \vec{B}$ . This implies  $B^2 = \vec{B}^2(1 - v^2) + (\mathbf{v} \cdot \vec{B})^2$ .

<sup>2</sup>Note that this form of the energy-momentum tensor is different from the one normally used in general-relativistic formulations of the equations of MHD. In particular, in that notation  $b^\mu$  are the contravariant components of the magnetic field in the frame comoving with the fluid; see Appendix A of Ref. [41] for a more detailed discussion.

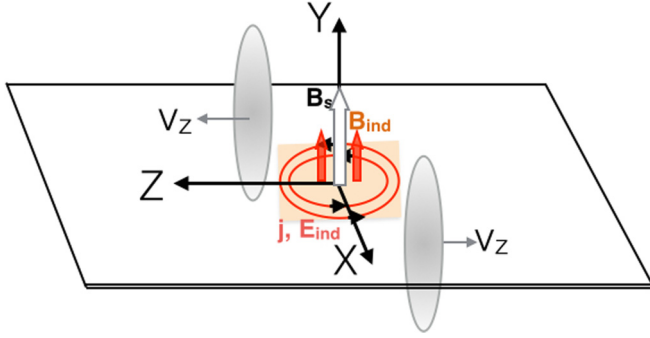


FIG. 1. Schematic diagram of a typical noncentral heavy-ion collision and the corresponding electromagnetic fields in the reaction zone.

Note also that the magnetization in the comoving frame is actually defined as  $M^\mu := \chi H^\mu = \chi B^\mu / (1 + \chi)$ , where  $H^\mu = B^\mu - M^\mu$  is the magnetic field in the comoving frame and  $\chi = \chi_B / (1 - \chi_B)$  is the magnetic susceptibility. If the latter is very small, then to first order  $\chi \simeq \chi_B$ , and the magnetization can be approximated as  $M^\mu \simeq \chi B^\mu + O(\chi^2)$ . Since the magnetic susceptibility  $\chi \ll 1$  in the temperature range applicable for heavy-ion collisions, i.e.,  $\chi \lesssim 0.05$  for  $eB \sim 0.2 \text{ GeV}^2$  [57], we will set  $M = 0$  in the actual calculations.

### C. Reduced-MHD evolution

As discussed above, a consistent MHD evolution would require us to solve Maxwell's equations (14) simultaneously with the energy-momentum conservation equation (1). In this work, we do not attempt this rather formidable task, but restrict ourselves to the so-called reduced-MHD setup, where the magnetic field evolution is prescribed from outside and only the energy-momentum conservation equation is solved.

The evolution of magnetic field considered here follows that of Ref. [2]. The physical picture is the following: although the magnetic field produced at the time of collisions is large, it also decays very quickly due to the high velocity of the spectators. According to the Maxwell equation  $\nabla \times \vec{E} = -\partial_t \vec{B}$ , a time-varying magnetic field induces an electric field, which, in turn, will produce an electric current  $\vec{j}$  in the QGP medium, which depends on the conductivity and the displacement current in the medium. This induced current will give rise to an induced magnetic field in the same direction as the original magnetic field and hence the net magnetic field is expected to decay more slowly than if the evolution took place in vacuum.

The physical conditions just described above are shown schematically in Fig. 1. The initial large but time-varying magnetic field produced mostly due to the spectators is shown as  $\vec{B}_s$ , whereas the induced magnetic field is shown by red arrows and denoted as  $\vec{B}_{\text{ind}}$ . The induced electric field in the reaction plane and the corresponding current  $\vec{j}$  are shown by the red circles. We remark that the calculation of Ref. [2] assumes a constant electric conductivity, but in our case the system evolves in space and time, so that the electrical conductivity of the plasma should not be taken to be constant but a function of temperature.

At this point, let us briefly comment on the treatment of the conservation equations in Ref. [38]. A common feature to our work is that the authors of Ref. [38] also assumed an ideally conducting fluid,  $E^\mu \rightarrow 0$ . There are, however, two important differences to our work: (i) the magnetization  $M$  was assumed to be nonzero and (ii) the effect of the magnetic field  $B$  in the energy-momentum conservation equation was neglected. In essence, Ref. [38] just solved the evolution equation (16) for the matter part of the energy-momentum tensor under the assumption of a vanishing electric-charge four-current  $j^\mu = 0$ , but for nonvanishing magnetization  $M$ . In this case, using the relations

$$M^\nu = M b^\nu, \quad B^\nu = B b^\nu, \quad b^\nu b_\nu = -1, \quad (21)$$

such that  $b^\nu \partial^\mu b_\nu = 0$ , Eq. (16) then reads

$$\partial_\nu T_{\text{mat}}^{\mu\nu} = -M \partial^\mu B. \quad (22)$$

Equation (22) differs by a sign from Eqs. (2) and (3) of Ref. [38]. However, note that the EOS of state used in the fluid evolution in Ref. [38] did not include the effect from the magnetic field. As discussed in Ref. [55], in this case one needs to replace  $\varepsilon \rightarrow \varepsilon - MB$ ,  $p \rightarrow p + MB$ , such that the right-hand side of Eq. (22) is replaced by  $+B \partial^\mu M$ . For a constant magnetic susceptibility  $\chi$ , this is then equivalent to Eq. (4) of Ref. [38]. However, that work used a temperature-dependent  $\chi$ , cf. their Eq. (5).

### D. (2 + 1)-dimensional geometry

We will assume a Bjorken-scaling expansion in the longitudinal direction, so that, on account of boost invariance, we may restrict the discussion to the  $z = 0$  plane, where for reasons of symmetry  $u^z = 0$ . In this case, it is advantageous to use Milne coordinates  $(\tau, x, y, \eta)$ , where  $\tau := \sqrt{t^2 - z^2}$ ,  $\eta := (1/2) \ln[(t+z)/(t-z)]$ , and the metric tensor is given by  $g^{\mu\nu} = \text{diag}(1, -1, -1, -1/\tau^2)$ . The energy-momentum conservation equations (1) then take the following form:

$$\partial_\tau \tilde{T}^{\tau\tau} + \partial_x (\tilde{T}^{\tau\tau} \tilde{v}^x) + \partial_y (\tilde{T}^{\tau\tau} \tilde{v}^y) = -p_B + \tau f_B \tilde{B}^2 (b^\eta)^2, \quad (23)$$

$$\partial_\tau \tilde{T}^{\tau x} + \partial_x (\tilde{T}^{\tau x} v^x) + \partial_y (\tilde{T}^{\tau x} v^y) = -\partial_x [\tilde{p}_B - f_B \tilde{B}^2 b^x (b^x - b^\tau v^x)] + \partial_y [f_B \tilde{B}^2 b^x (b^y - b^\tau v^y)], \quad (24)$$

$$\partial_\tau \tilde{T}^{\tau y} + \partial_x (\tilde{T}^{\tau y} v^x) + \partial_y (\tilde{T}^{\tau y} v^y) = -\partial_y [\tilde{p}_B - f_B \tilde{B}^2 b^y (b^y - b^\tau v^y)] + \partial_x [f_B \tilde{B}^2 b^y (b^x - b^\tau v^x)], \quad (25)$$

where we have defined

$$p_B := p - MB + \frac{B^2}{2}, \quad f_B := 1 - \frac{M}{B}, \quad (26)$$

as well as  $\tilde{T}^{\mu\nu} := \tau T^{\mu\nu}$ ,  $\tilde{p}_B := \tau p_B$ ,  $\tilde{B}^2 := \tau B^2$ , and

$$\tilde{v}^x := \frac{T^{x\tau}}{T^{\tau\tau}} = \frac{w\gamma^2 v^x - f_B B^2 b^x b^\tau}{w\gamma^2 - p_B - f_B B^2 (b^\tau)^2}, \quad (27)$$

$$\tilde{v}^y := \frac{T^{y\tau}}{T^{\tau\tau}} = \frac{w\gamma^2 v^y - f_B B^2 b^y b^\tau}{w\gamma^2 - p_B - f_B B^2 (b^\tau)^2}, \quad (28)$$

with  $w := \varepsilon + p + f_B B^2$ . Note that, at  $\eta = 0$ ,  $b^i - b^\tau v^i = \tilde{B}^i / (\gamma B)$ . Note also that, at  $\eta = 0$ ,  $b^\eta = \tilde{B}^z / (\gamma B)$ , which vanishes if the magnetic field  $\tilde{\mathbf{B}}$  has no component in beam direction.

From Eq. (25) it is clear that a magnetic field along the  $y$  direction decreases the total pressure. However, since what drives the evolution of the fluid are the pressure gradients, a constant magnetic field does not lead to a change of the fluid acceleration. That said, and we will see below, the spatial distribution of the magnetic field is such that also pressure gradients are enhanced (reduced) along the  $x$  ( $y$ ) axis, respectively. Ultimately, this will result in an increase in the momentum-space anisotropy of the fluid.

The set of equations (23)–(25) is closed by an EOS and we use the EOS indicated as s95p-PCE165-v0 in Refs. [58,59], which is constructed from lattice-QCD data at high temperature and a partially chemically equilibrated hadron resonance gas at low temperature. From now on we will refer to this as EOS-LHRG. Note that, for  $M = 0$ , neither  $\varepsilon$  nor  $p$  change due to a nonvanishing magnetization energy density.

### III. NUMERICAL SETUP

We solve the conservation equations (23)–(25) for  $M = 0$ , i.e.,  $f_B \equiv 1$ , by using an appropriately modified (see below) version of the publicly available (2 + 1)-dimensional perfect fluid dynamics code AZHYDRO [60,61], which uses the multidimensional flux-correcting algorithm SHASTA to solve the energy-momentum conservation equations.

At each time step the conserved quantities  $T^{\tau\tau}$ ,  $T^{x\tau}$ , and  $T^{y\tau}$  are evolved to the next time step using the SHASTA algorithm. In order to find the primitive variables  $\varepsilon$ ,  $p$ ,  $v^x$ ,  $v^y$  from the time-evolved conserved quantities we use the following algorithm [62]. First we define the quantities

$$\mathcal{E} := T^{\tau\tau} = w\gamma^2 - p_B - B^2 (b^\tau)^2, \quad (29)$$

$$\mathcal{M}^x := T^{\tau x} = w\gamma^2 v^x - B^2 b^\tau b^x, \quad (30)$$

$$\mathcal{M}^y := T^{\tau y} = w\gamma^2 v^y - B^2 b^\tau b^y. \quad (31)$$

Note that the momentum flow vector  $\mathcal{M} = (\mathcal{M}^x, \mathcal{M}^y)$  is not always parallel to the fluid velocity vector  $\mathbf{v} = (v^x, v^y)$  and thus we cannot apply the algorithm given in the original AZHYDRO code to find the new velocity. To counter this problem we next introduce the new quantities

$$\mathcal{E}' := \mathcal{E} + B^2 (b^\tau)^2 = w\gamma^2 - p_B, \quad (32)$$

$$\mathcal{M}^{x'} := \mathcal{M}^x + B^2 b^\tau b^x = w\gamma^2 v^x, \quad (33)$$

$$\mathcal{M}^{y'} := \mathcal{M}^y + B^2 b^\tau b^y = w\gamma^2 v^y, \quad (34)$$

where the new three-vector  $\mathcal{M}' = (\mathcal{M}^{x'}, \mathcal{M}^{y'})$  is always parallel to  $\mathbf{v}$ . As a result, we can now apply the well-known technique (given below) of finding primitive variables at each

time step. More specifically, after defining  $\mathcal{M}' := |\mathcal{M}'|$  and  $v := |\mathbf{v}|$ , we can write

$$\mathcal{M}' = (\mathcal{E}' + p_B)v, \quad (35)$$

$$\varepsilon = \mathcal{E}' - \mathcal{M}'v - \frac{B^2}{2}, \quad (36)$$

and use the above expressions to replace  $\varepsilon$  in  $p(\varepsilon)$  to finally obtain

$$v = \frac{\mathcal{M}'}{\mathcal{E}' + p(\varepsilon)} \Big|_{\varepsilon = \mathcal{E}' - \mathcal{M}'v - B^2/2}. \quad (37)$$

For given values of  $\mathcal{E}'$ ,  $\mathcal{M}'$ , and  $B^2$ , Eq. (37) can be solved iteratively for the velocity  $v$ , which, once known, allows us to compute  $\varepsilon$  from Eq. (36). Finally, the distinct components  $v^x$  and  $v^y$  can be obtained from the collinearity of  $\mathcal{M}'$  and  $\mathbf{v}$ .

#### A. Initial data

Obviously, in order to solve the system of coupled partial differential equations (23)–(25) a set of initial conditions needs to be specified. In particular, at the initial time of the hydrodynamical evolution, which we choose as  $\tau_0 = 0.6$  fm, we set  $v^x = v^y = 0$ , while the initial energy density in the transverse plane is obtained from the Glauber model via the following two-component form

$$\varepsilon(x, y, b) = \varepsilon_0 [x_h N_{\text{part}}(x, y, b) + (1 - x_h) N_{\text{coll}}(x, y, b)]. \quad (38)$$

Here,  $N_{\text{part}}(x, y, b)$  and  $N_{\text{coll}}(x, y, b)$  are the transverse profiles of the average number of participants and the average number of binary collisions, respectively, both calculated within a Glauber model for a given impact parameter  $b$ . The fraction of hard scattering  $x_h$  is important to explain the centrality dependence of the average charged hadron multiplicity. Since we will not compare our result to experimental data, we take  $x_h = 0.25$  in all cases considered.

#### B. Magnetic-field evolution

In a fully consistent solution of the MHD equations with appropriate boundary conditions the induction equation would provide the evolution of the magnetic field as a result of the dynamics of the magnetized flow. However, as mentioned in Sec. I, we here employ a reduced set of MHD equations, and the evolution of the external magnetic field is taken to follow some suitably defined function in space and time. Inspired by a previous study [44], we use the following parametrized form in space and time for the  $y$  component of the magnetic field

$$\frac{e\tilde{B}^y(x, y, \tau)}{m_\pi^2} = f(\tau) \exp \left[ -\frac{(x - x_0)^2}{4\sigma_x^2} - \frac{(y - y_0)^2}{4\sigma_y^2} \right]. \quad (39)$$

In all cases considered we center the Gaussian in Eq. (39) at  $x_0 = y_0 = 0$  and use  $\sigma_x$ ,  $\sigma_y$  to set the widths of the Gaussian in  $x$  and  $y$  direction, respectively. For an impact parameter  $b = 0$ , we use  $\sigma_x = \sigma_y = 3.5$  fm, while for  $b = 10$  fm, we set  $\sigma_x = 1.5$  fm and  $\sigma_y = 2.2$  fm. The corresponding magnetic

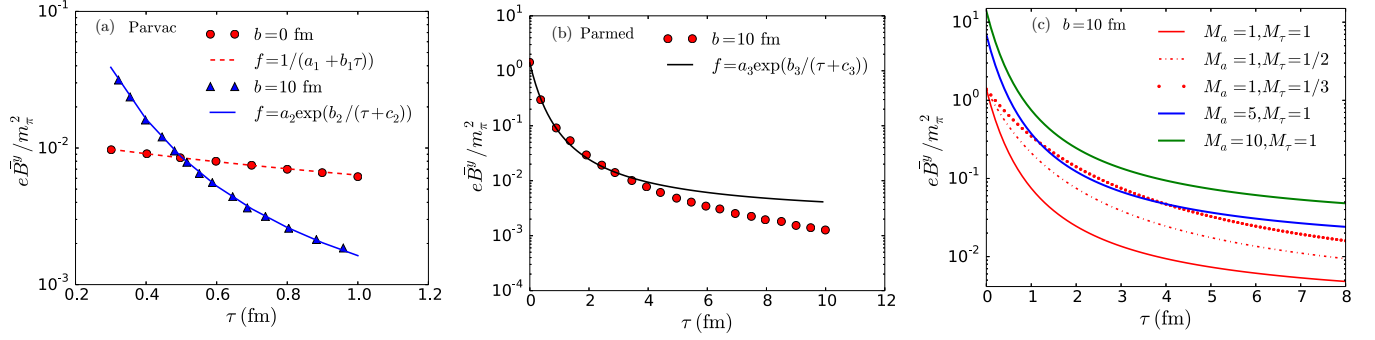


FIG. 2. Evolution of  $e\bar{B}^y$ , normalized to the pion mass squared at  $x = y = 0$ . (a) Evolution of  $e\bar{B}^y$  in vacuum, for  $b = 0$  fm collisions (red circles and line), and for  $b = 10$  fm collisions (blue triangles and line). The values corresponding to symbols are taken from Ref. [1], the lines are fits, respectively. (b) Evolution of  $e\bar{B}^y$  in medium with a finite conductivity for  $b = 10$  fm collisions, red open circles are from Ref. [2], the black solid line is a fit. (c) The same as middle panel, but for various values of the fit parameters.

energy densities at  $\tau = 0$  are shown in Fig. 3 for the cases of  $b = 0$  (left panel) and  $b = 10$  fm (right panel).

The evolution of the magnetic field in the QGP is not well known. In vacuum, the decay time of the magnetic field is inversely proportional to the  $\sqrt{s_{NN}}$  of the collision [1]. However, several studies have shown that the QGP possesses a nonzero temperature-dependent electrical conductivity [63–65]. In this case, the decay of the magnetic field can be substantially delayed [5,46].

In view of these considerations and uncertainties, we here employ a function of proper time only, i.e.,  $f(\tau)$  in Eq. (39), as a fully phenomenological ansatz for a reasonable parametrization of the evolution of the magnetic field  $\bar{B}^y$ , distinguishing the case in which the field is in vacuum from when it is in a QGP.

- (i) In vacuum we parametrize the evolution of the magnetic field as in Ref. [1], so that for  $b = 0$  fm collisions

$$f(\tau) = \frac{1}{a_1 + b_1\tau}, \quad (40)$$

and for  $b = 10$  fm collisions

$$f(\tau) = a_2 e^{b_2/(\tau+c_2)}. \quad (41)$$

Adjusting the constants in these parametrizations to the data given in Ref. [1], we obtain  $a_1 = 78.2658$ ,  $b_1 = 79.5457 \text{ fm}^{-1}$ ,  $a_2 = 1.357 \times 10^{-4}$ ,  $b_2 = 3.1031 \text{ fm}$ , and  $c_2 = 0.2483 \text{ fm}$ . The data are shown by the symbols in Fig. 2(a), while our parametrizations (40) and (41) are given by the lines in that figure. From now on we denote these parametrizations as Parvac, since they are valid in vacuum.

- (ii) In a QGP with nonzero electrical conductivity we parametrize the evolution of the magnetic field as in Ref. [2] [see Fig. 3 of Ref. [2]]

$$f(\tau) = M_a a_3 e^{b_3/(M_\tau \tau + c_3)}. \quad (42)$$

We denote this parametrization as Parmed. Data from Ref. [2] are shown in Fig. 2(b). We fit these data setting  $M_a = M_\tau = 1$  and adjusting the constants, giving  $a_3 = 1.99 \times 10^{-3}$ ,  $b_3 = 8.1306 \text{ fm}$ , and  $c_3 = 1.2420 \text{ fm}$ . We note that at late times, i.e., for  $\tau \geq 5 \text{ fm}$ , the fit (black line) overestimates the corresponding data points (open red circles), but also that the magnetic field at this time is already two orders of magnitude smaller than its initial value, so that this mismatch is likely not dynamically important.

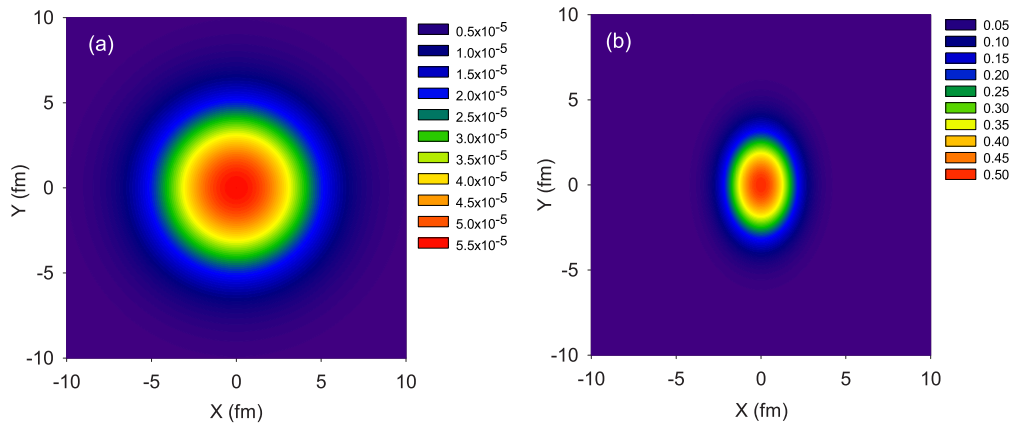


FIG. 3. Magnetic-field energy density in the transverse plane at  $\tau = 0$  fm. (a) refers to collisions with  $b = 0$  fm, while (b) to collisions with  $b = 10$  fm.

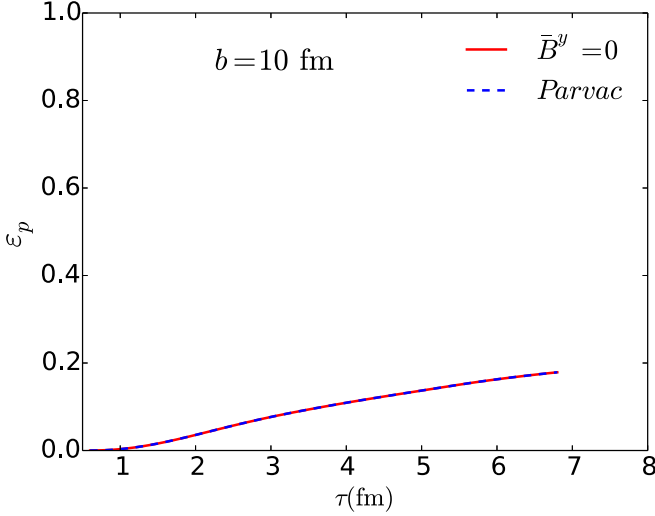


FIG. 4. Evolution of the momentum anisotropy  $\varepsilon_p$  for  $b = 10$  fm collisions when the magnetic field is taken to be zero (solid red line) or to follow the Parvac parametrization (dashed blue line).

As an extension of the space of parameters we have also studied variations of the parametrization (42) by changing the constants  $M_a$  and  $M_\tau$ . Since varying  $M_a$  changes the value of  $\bar{B}^y$  at  $\tau = 0$ , we have considered  $M_a = 1, 5$ , and  $10$ , which corresponds to  $e\bar{B}^y/m_\pi^2 \sim 1, 5$ , and  $10$  at  $\tau = 0$ , respectively. Furthermore, the decay rate has been varied by using different values of  $M_\tau$  and for each value of  $M_a$  we use three different values, namely,  $M_\tau = 1, 1/2$ , and  $1/3$ .

#### IV. RESULTS

In order to measure the effect of a strong magnetic field we investigate the evolution of the momentum anisotropy of the fluid flow in Au+Au collisions and defined as

$$\varepsilon_p(\tau) := \frac{\langle T^{xx} - T^{yy} \rangle}{\langle T^{xx} + T^{yy} \rangle}, \quad (43)$$

where  $\langle \dots \rangle$  denotes the energy-density weighted average over the transverse plane at proper time  $\tau$ , i.e., for a

generic component

$$\langle T^{ij}(\tau) \rangle := \frac{\int dx dy \varepsilon(x, y, \tau) T^{ij}(x, y, \tau)}{\int dx dy \varepsilon(x, y, \tau)}. \quad (44)$$

The momentum anisotropy is a particularly interesting quantity to study since an azimuthally asymmetric energy-density distribution in the transverse plane in noncentral collisions is expected to give rise to stronger pressure gradients along the  $x$  direction than along the  $y$  direction, at least in our geometrical setup. In turn, since pressure gradients drive the fluid flow, a momentum anisotropy of this type is directly related to a higher flow velocity along the  $x$  direction than along the  $y$  direction. In Ref. [60] it was shown that  $\varepsilon_p$  at freeze out is directly related to the transverse-momentum squared ( $p_T^2$ ) weighted elliptic flow of pions. Thus, any change in  $\varepsilon_p$  also indicates a possible change in the elliptic flow of hadrons and the following results corroborate this expectation.

As an initial test of the numerical infrastructure we have considered the simplified but also physically less interesting case of central collisions, i.e.,  $b = 0$ . In this case, the symmetry of the system yields  $\varepsilon_p = 0$  at all times in a purely hydrodynamical flow. Actually, this result applies also in the presence of a magnetic field, since the magnetic-field contribution in the  $x$  direction is expected to be the same as the one in the  $y$  direction, at least when  $b = 0$ . However, our numerical setup, in which only  $\bar{B}^y$  is switched on, does not allow us to validate this behavior, but we have verified that the growth of  $\varepsilon_p$  is nevertheless extremely small, being  $\varepsilon_p \lesssim 10^{-6}$  for a Parvac parametrization and  $\varepsilon_p \lesssim 2 \times 10^{-3}$  for a Parmed parametrization with  $M_a = 5$ .

On the other hand, for peripheral collisions one expects an anisotropy to develop already from the underlying asymmetric hydrodynamical flow. This anisotropy can then be further amplified if a magnetic field is present. Figure 4 shows the growth of such anisotropy by reporting the evolution of  $\varepsilon_p$  for a collision with  $b = 10$  fm. Shown with a solid red line is the purely hydrodynamical evolution (i.e., with zero magnetic field), while the dashed blue line refers to the Parvac parametrization. Clearly the two curves are very similar and this is essentially because with the parametrization (41) the magnetic field is effectively very small,  $e\bar{B}^y/m_\pi^2 \lesssim 10^{-2}$  [cf. Fig. 2(a)].

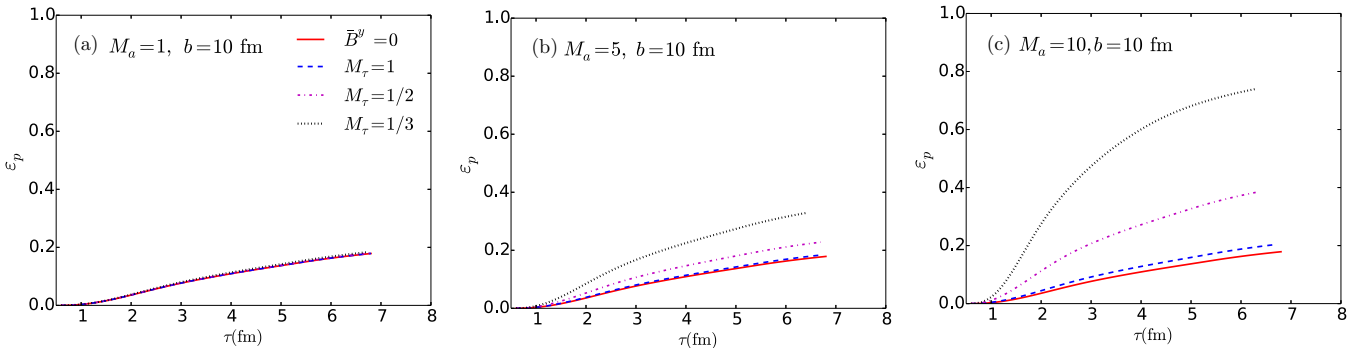


FIG. 5. Evolution of the momentum anisotropy for  $b = 10$  fm collisions for the Parmed case. (a) The solid red line corresponds to the result for zero magnetic field, the dashed blue, dash-dotted magenta, and dotted black lines correspond to results with external magnetic field for  $M_\tau = 1, 1/2$ , and  $1/3$ , respectively; in all cases  $M_a = 1$ . (b) The same as in (a), but for  $M_a = 5$ . (c) The same as in (a), but for  $M_a = 10$ .

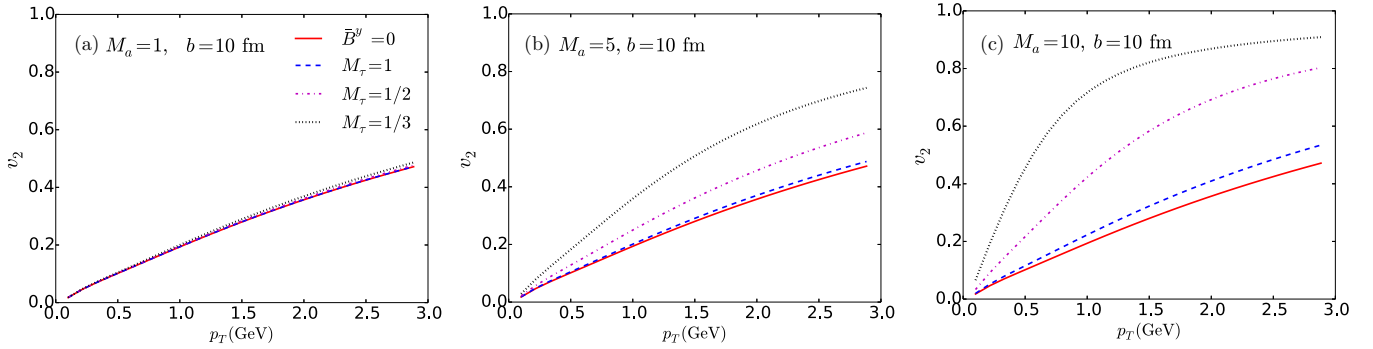


FIG. 6. The elliptic-flow coefficient  $v_2$  for  $\pi^-$  as a function of transverse momentum  $p_T$  for  $b = 10$  fm collisions. (a) The solid red line corresponds to the result for zero magnetic field, the dashed blue, dash-dotted magenta, and dotted black lines correspond to results for an external magnetic field with  $M_\tau = 1, 1/2$ , and  $1/3$ , respectively. All results are obtained for  $M_a = 1$ . (b) The same as in (a), but for  $M_a = 5$ . (c) The same as in (a), but for  $M_a = 10$ .

The evolution of the momentum anisotropy  $\varepsilon_p$  for the case of collisions with  $b = 10$  fm and when the magnetic field is evolved using the Parmed parametrization is shown in Fig. 5. More specifically, Fig. 5(a) corresponds to the case where the initial magnetic-field amplitude is  $M_a = 1$ , i.e., when the magnetic field at  $\tau = 0$  is set to be  $e\bar{B}^y \sim m_\pi^2$ . The solid red line corresponds to the case without magnetic field, while the dashed blue, dash-dotted magenta, and dotted black lines correspond to  $M_\tau = 1, 1/2$ , and  $1/3$ , respectively. The evolution is shown up to freeze out, that is when the temperature is nowhere larger than  $T_f = 130$  MeV.

A rapid inspection of Fig. 5(a) reveals that a visible change in  $\varepsilon_p$  is seen only when the magnetic field decays very slowly, i.e., for  $M_\tau = 1/3$  (dotted black line). Under these conditions one is induced to conclude that the influence of the magnetic field is very limited and that the momentum anisotropy remains small, with a relative variation relative to the purely hydrodynamical case of  $|1 - \varepsilon_p/\varepsilon_p(\bar{B}^y = 0)| \lesssim 3 \times 10^{-2}$ . However, because the common expectation is that the initial magnetic field in  $b = 10$  fm Au+Au collisions can be substantially larger than  $m_\pi^2$ , Fig. 5(b) reports the evolution of the momentum anisotropy for a larger initial magnetic field, i.e.,  $M_a = 5$  or  $e\bar{B}^y \simeq 5 m_\pi^2$  at  $\tau = 0$ . In this case, in fact, even for the most rapid decay of the magnetic field, i.e.,  $M_\tau = 1$ , the momentum anisotropy  $\varepsilon_p$  is larger when compared to the case of zero magnetic field; the largest relative difference in this case is  $|1 - \varepsilon_p/\varepsilon_p(\bar{B}^y = 0)| \sim 0.8$  and is obviously obtained for  $M_\tau = 1/3$ . Finally, as can be seen from Fig. 5(c), a much higher initial value of the magnetic field (i.e.,  $M_a = 10$ ) increases  $\varepsilon_p$  even more, with a relative difference that can now be  $|1 - \varepsilon_p/\varepsilon_p(\bar{B}^y = 0)| \sim 3.2$  for  $M_\tau = 1/3$ .

As mentioned earlier, the elliptic-flow coefficient  $v_2$  of charged hadrons is directly proportional to the momentum anisotropy  $\varepsilon_p$ , so that we expect also a noticeable change of  $v_2$  due to the magnetic field. For demonstration purposes, we show here  $v_2$  of  $\pi^-$  only.<sup>3</sup> Since we are not trying to match experimental data, the input parameters for simulations

are not adjusted to reproduce any experimentally measured charged-hadron multiplicity. However, we do use realistic values for the input parameters corresponding to Au+Au collisions at  $\sqrt{s_{NN}} = 200$  GeV. More specifically, at the initial time  $\tau_0 = 0.5$  fm and for central collisions ( $b = 0$  fm) we set the central energy density to be  $\varepsilon = 50$  GeV fm<sup>-3</sup> and consider a constant freeze-out temperature of 120 MeV. However, neither resonance decays nor viscous corrections are taken into account.

Figure 6 shows the elliptic-flow coefficient  $v_2$  of  $\pi^-$  as a function of the transverse momentum  $p_T$  for noncentral collisions with  $b = 10$  fm. Different lines refer to the same set of conditions as in Fig. 5, namely, the solid red line corresponds to the result for zero magnetic field, the dashed blue, dash-dotted magenta, and dotted black lines correspond to results with external magnetic field for  $M_\tau = 1, 1/2$ , and  $1/3$ , respectively. In analogy with what we discussed for the momentum anisotropy, it is clear from Fig. 6 that changes in  $v_2$  are noticeable only when either the initial magnetic field is large or when the magnetic field decay is substantially delayed. For the largest initial value of the magnetic field considered here, i.e., for  $e\bar{B}^y \simeq 10 m_\pi^2$ , we notice a considerable enhancement of the elliptic-flow coefficient, which can become as large as  $v_2 \lesssim 0.9$  for  $p_T \sim 2.5$  GeV [cf. dotted black line in Fig. 6(c)]. A smaller initial magnetic field, i.e.,  $e\bar{B}^y \simeq 5 m_\pi^2$ , leads to a smaller increase of the elliptic-flow coefficient, which however remains rather large, with  $v_2 \lesssim 0.7$  for  $p_T \sim 2.5$  GeV [cf. dotted black line in Fig. 6(b)], thus highlighting that quite realistic values of the magnetic field can have a considerable impact on the ellipticity of the flow of particles. Overall, these results and their implications for the understanding of the physics of ultrarelativistic heavy-ion collisions clearly call for the extension of this study towards a fully self-consistent MHD treatment of the evolution of hot and dense strongly interacting matter created in heavy-ion collisions, following the spirit of the work in Ref. [50].

## V. CONCLUSIONS

We have investigated the effect of a strong external magnetic field on the evolution of matter created in  $\sqrt{s_{NN}} = 200$  GeV Au+Au collisions within a (2 + 1)-dimensional

<sup>3</sup>Note that elliptic-flow coefficient  $v_2$  for  $\pi^+$  would be identical, since any effect of the magnetic field after freeze out is neglected.

reduced-MHD description. In particular, we have assumed that the external magnetic field has only a nonvanishing component transverse to the reaction plane (i.e., it is aligned with the  $y$  direction) and we have employed the space-time variation suggested in Refs. [1,2]. Overall and on average, we found no visible changes in the fluid-velocity profile when comparing the magnetic-field decays in vacuum with the case in which the magnetic field is actually zero.

On the other hand, a substantial change in the fluid velocity and, consequently, in the elliptic-flow coefficient  $v_2$  of  $\pi^-$  is observed when the magnetic field is sufficiently large, i.e., for  $e\bar{B}^y \gtrsim 5m_\pi^2$ , or when a nonzero electrical conductivity of the QGP is accounted for such that it decays slowly, i.e., for  $M_\tau \gtrsim 1/2$ . Under these conditions, the momentum anisotropy shows a relative variation relative to the purely hydrodynamical case of  $|1 - \varepsilon_p/\varepsilon_p(\bar{B}^y = 0)| \gtrsim 1/2$ , while the elliptic-flow coefficient can become as large as  $v_2 \sim 0.7$  for  $p_T \sim 2.5$  GeV (all of the values reported refer to an initial magnetic field strength  $e\bar{B}^y \simeq 5m_\pi^2$ ).

Our results are obtained under some simplifying assumptions: (i) We have used an analytic prescription for the magnetic-field evolution, but the latter should really be the result of a self-consistent solution of the full set of ideal-MHD equations [50]. (ii) We have considered event-averaged values for the initial energy density and the magnetic field, but both of them fluctuate event to event in reality. Indeed, a previous study [44] has shown that because of the event-by-event fluctuations of both the magnetic energy density and of the fluid energy density, in some cases the ratio of these two quantities can be  $\sim 1$ . In such cases, the magnetic field will have a larger effect than considered here. (iii) We have neglected the  $x$  component of the magnetic field as we expect that  $\bar{B}^x \ll \bar{B}^y$  in the present geometrical setup. Although this is a good approximation for peripheral collisions, in central collisions  $\bar{B}^x$  is of the same order as  $\bar{B}^y$  and one needs to consider both. (iv) We have considered a decay of the magnetic field pertaining to a constant electrical conductivity [2]. However, one should use the appropriate temperature-dependent electri-

cal conductivity of the QGP. (v) We have considered the case of vanishing magnetization, but, depending on the magnetic properties of the QGP and the hadronic phase, a nonzero magnetization of the medium needs to be accounted for in the full energy-momentum tensor, as some recent preliminary studies show that this could also affect the QGP evolution [38,42]. (vi) We have considered here only perfect fluids [49], but it is important to take into account also dissipative corrections to the fluid evolution. Nonzero magnetic fields will have an impact on the value of the shear viscosity-to-entropy density ratio  $\eta_{\text{sh}}/s$  extracted from a comparison to experimental data, as was also speculated in some previous studies [45,46].

Overall, we regard the present study as being of exploratory nature. In addition to the considerations made above and together with a systematic exploration of the input parameters, our work will need to be extended in a number of ways. These include: the study of the corrections to the final particle spectra due to the magnetic field at and after freeze out; the study of several other experimental observables, e.g., charge-dependent azimuthal correlations and soft-photon production [66–69]; as well as the investigation of smaller collision energies, where the decay of the magnetic field is slower and thus its impact on the fluid evolution is expected to be more pronounced.

## ACKNOWLEDGMENTS

It is a pleasure to thank Gergely Endrödi, Xu-Guang Huang, Igor Mishustin, Long-Gang Pang, and Hannah Petersen for discussions and comments. V.R. is supported by the DST-INSPIRE faculty research grant. S.P. is supported by a JSPS postdoctoral fellowship for foreign researchers. D.H.R. is partially supported by the High-end Foreign Experts project GDW20167100136 of the State Administration of Foreign Experts Affairs of China. Support also comes from “New-CompStar”, COST Action MP1304, and from the LOEWE program HIC for FAIR.

- 
- [1] W. T. Deng and X. G. Huang, Event-by-event generation of electromagnetic fields in heavy-ion collisions, *Phys. Rev. C* **85**, 044907 (2012).
  - [2] K. Tuchin, Time and space dependence of the electromagnetic field in relativistic heavy-ion collisions, *Phys. Rev. C* **88**, 024911 (2013).
  - [3] A. Bzdak and V. Skokov, Event-by-event fluctuations of magnetic and electric fields in heavy ion collisions, *Phys. Lett. B* **710**, 171 (2012).
  - [4] K. Tuchin, Electromagnetic field and the chiral magnetic effect in the quark-gluon plasma, *Phys. Rev. C* **91**, 064902 (2015).
  - [5] H. Li, X. L. Sheng, and Q. Wang, Electromagnetic fields with electric and chiral magnetic conductivities in heavy ion collisions, *Phys. Rev. C* **94**, 044903 (2016).
  - [6] K. Tuchin, Synchrotron radiation by fast fermions in heavy-ion collisions, *Phys. Rev. C* **82**, 034904 (2010); [**83**, 039903(E) (2011)].
  - [7] K. Tuchin, Photon decay in strong magnetic field in heavy-ion collisions, *Phys. Rev. C* **83**, 017901 (2011).
  - [8] G. Basar, D. E. Kharzeev, and V. Skokov, Conformal Anomaly as a Source of Soft Photons in Heavy Ion Collisions, *Phys. Rev. Lett.* **109**, 202303 (2012).
  - [9] D. E. Kharzeev, L. D. McLerran, and H. J. Warringa, The effects of topological charge change in heavy ion collisions: “Event by event P and CP violation”, *Nucl. Phys. A* **803**, 227 (2008).
  - [10] Y. Hirono, T. Hirano, and D. E. Kharzeev, The chiral magnetic effect in heavy-ion collisions from event-by-event anomalous hydrodynamics, [arXiv:1412.0311](https://arxiv.org/abs/1412.0311) [hep-ph].
  - [11] D. T. Son and N. Yamamoto, Berry Curvature, Triangle Anomalies, and the Chiral Magnetic Effect in Fermi Liquids, *Phys. Rev. Lett.* **109**, 181602 (2012).
  - [12] D. T. Son and N. Yamamoto, Kinetic theory with Berry curvature from quantum field theories, *Phys. Rev. D* **87**, 085016 (2013).

- [13] M. A. Stephanov and Y. Yin, Chiral Kinetic Theory, *Phys. Rev. Lett.* **109**, 162001 (2012).
- [14] J. H. Gao, Z. T. Liang, S. Pu, Q. Wang, and X. N. Wang, Chiral Anomaly and Local Polarization Effect from Quantum Kinetic Approach, *Phys. Rev. Lett.* **109**, 232301 (2012).
- [15] J. W. Chen, S. Pu, Q. Wang, and X. N. Wang, Berry Curvature and Four-Dimensional Monopoles in the Relativistic Chiral Kinetic Equation, *Phys. Rev. Lett.* **110**, 262301 (2013).
- [16] Y. Hidaka, S. Pu, and D. L. Yang, Relativistic chiral kinetic theory from quantum field theories, *Phys. Rev. D* **95**, 091901 (2017).
- [17] S. Pu, S. Y. Wu, and D. L. Yang, Chiral hall effect and chiral electric waves, *Phys. Rev. D* **91**, 025011 (2015).
- [18] J. W. Chen, T. Ishii, S. Pu, and N. Yamamoto, Nonlinear chiral transport phenomena, *Phys. Rev. D* **93**, 125023 (2016).
- [19] S. Ebihara, K. Fukushima, and S. Pu, Boost invariant formulation of the chiral kinetic theory, *Phys. Rev. D* **96**, 016016 (2017).
- [20] E. V. Gorbar, I. A. Shovkovy, S. Vilchinskii, I. Rudenok, A. Boyarsky, and O. Ruchavskiy, Anomalous Maxwell equations for inhomogeneous chiral plasma, *Phys. Rev. D* **93**, 105028 (2016).
- [21] A. Bhattacharyya, S. K. Ghosh, R. Ray, and S. Samanta, Exploring effects of magnetic field on the hadron resonance gas, *Europhys. Lett.* **115**, 62003 (2016).
- [22] B. McNnes, A rotation/magnetism analogy for the quark–gluon plasma, *Nucl. Phys. B* **911**, 173 (2016).
- [23] D. E. Kharzeev, The chiral magnetic effect and anomaly-induced transport, *Prog. Part. Nucl. Phys.* **75**, 133 (2014).
- [24] A. Bzdak, V. Koch, and J. Liao, Charge-dependent correlations in relativistic heavy ion collisions and the chiral magnetic effect, *Lect. Notes Phys.* **871**, 503 (2013).
- [25] D. E. Kharzeev, Topology, magnetic field, and strongly interacting matter, *Ann. Rev. Nucl. Part. Sci.* **65**, 193 (2015).
- [26] K. Tuchin, Particle production in strong electromagnetic fields in relativistic heavy-ion collisions, *Adv. High Energy Phys.* **2013**, 490495 (2013).
- [27] X. G. Huang, Electromagnetic fields and anomalous transports in heavy-ion collisions—a pedagogical review, *Rep. Prog. Phys.* **79**, 076302 (2016).
- [28] C. Shen, S. A. Bass, T. Hirano, P. Huovinen, Z. Qiu, H. Song, and U. Heinz, The QGP shear viscosity: Elusive goal or just around the corner? *J. Phys. G* **38**, 124045 (2011).
- [29] P. Romatschke and U. Romatschke, *Phys. Rev. Lett.* **99**, 172301 (2007); M. Luzum and P. Romatschke, *Phys. Rev. C* **78**, 034915 (2008).
- [30] H. Song and U. W. Heinz, *Phys. Lett. B* **658**, 279 (2008); *Phys. Rev. C* **78**, 024902 (2008).
- [31] P. Bozek and I. Wyskiel-Piekarska, Particle spectra in Pb-Pb collisions at  $\sqrt{s_{NN}} = 2.76$  TeV, *Phys. Rev. C* **85**, 064915 (2012).
- [32] V. Roy, A. K. Chaudhuri, and B. Mohanty, Comparison of results from a 2+1D relativistic viscous hydrodynamic model to elliptic and hexadecapole flow of charged hadrons measured in Au-Au collisions at  $\sqrt{s_{NN}} = 200$  GeV, *Phys. Rev. C* **86**, 014902 (2012).
- [33] H. Niemi, G. S. Denicol, P. Huovinen, E. Molnar, and D. H. Rischke, Influence of a temperature-dependent shear viscosity on the azimuthal asymmetries of transverse momentum spectra in ultrarelativistic heavy-ion collisions, *Phys. Rev. C* **86**, 014909 (2012).
- [34] U. Heinz, C. Shen, and H. Song, The viscosity of quark-gluon plasma at RHIC and the LHC, *AIP Conf. Proc.* **1441**, 766 (2012).
- [35] B. Schenke, S. Jeon, and C. Gale, Higher flow harmonics from (3+1)D event-by-event viscous hydrodynamics, *Phys. Rev. C* **85**, 024901 (2012).
- [36] U. Gursoy, D. Kharzeev, and K. Rajagopal, Magnetohydrodynamics, charged currents and directed flow in heavy ion collisions, *Phys. Rev. C* **89**, 054905 (2014).
- [37] B. G. Zakharov, Electromagnetic response of quark-gluon plasma in heavy-ion collisions, *Phys. Lett. B* **737**, 262 (2014).
- [38] L. G. Pang, G. Endrödi, and H. Petersen, Magnetic-field-induced squeezing effect at energies available at the BNL Relativistic Heavy Ion Collider and at the CERN Large Hadron Collider, *Phys. Rev. C* **93**, 044919 (2016).
- [39] A. Das, S. S. Dave, P. S. Saumia, and A. M. Srivastava, Effects of magnetic field on plasma evolution in relativistic heavy-ion collisions, *Phys. Rev. C* **96**, 034902 (2017).
- [40] M. Greif, C. Greiner, and Z. Xu, Magnetic field influence on the early-time dynamics of heavy-ion collisions, *Phys. Rev. C* **96**, 014903 (2017).
- [41] V. Roy, S. Pu, L. Rezzolla, and D. Rischke, Analytic Bjorken flow in one-dimensional relativistic magnetohydrodynamics, *Phys. Lett. B* **750**, 45 (2015).
- [42] S. Pu, V. Roy, L. Rezzolla, and D. H. Rischke, Bjorken flow in one-dimensional relativistic magnetohydrodynamics with magnetization, *Phys. Rev. D* **93**, 074022 (2016).
- [43] S. Pu and D. L. Yang, Transverse flow induced by inhomogeneous magnetic fields in the Bjorken expansion, *Phys. Rev. D* **93**, 054042 (2016).
- [44] V. Roy and S. Pu, Event-by-event distribution of magnetic field energy over initial fluid energy density in  $\sqrt{s_{NN}} = 200$  GeV Au-Au collisions, *Phys. Rev. C* **92**, 064902 (2015).
- [45] R. K. Mohapatra, P. S. Saumia, and A. M. Srivastava, Enhancement of flow anisotropies due to magnetic field in relativistic heavy-ion collisions, *Mod. Phys. Lett. A* **26**, 2477 (2011).
- [46] K. Tuchin, On viscous flow and azimuthal anisotropy of quark-gluon plasma in strong magnetic field, *J. Phys. G* **39**, 025010 (2012).
- [47] R. Critelli, S. I. Finazzo, M. Zaniboni, and J. Noronha, Anisotropic shear viscosity of a strongly coupled non-Abelian plasma from magnetic branes, *Phys. Rev. D* **90**, 066006 (2014).
- [48] V. Voronyuk, V. D. Toneev, W. Cassing, E. L. Bratkovskaya, V. P. Konchakovski, and S. A. Voloshin, (Electro-)Magnetic field evolution in relativistic heavy-ion collisions, *Phys. Rev. C* **83**, 054911 (2011).
- [49] L. Rezzolla and O. Zanotti, *Relativistic Hydrodynamics* (Oxford University Press, Oxford, 2013).
- [50] G. Inghirami, L. Del Zanna, A. Beraudo, M. H. Moghaddam, F. Becattini, and M. Bleicher, Numerical magneto-hydrodynamics for relativistic nuclear collisions, *Eur. Phys. J. C* **76**, 659 (2016).
- [51] S. R. de Groot and L. G. Suttrop, *Foundations of Electrodynamics* (North-Holland, Amsterdam, 1972).
- [52] W. Israel, *Gen. Rel. Grav.* **9**, 451 (1978).
- [53] P. Kovtun, *J. High Energy Phys.* **07** (2016) 028.
- [54] M. Gedalin and I. Oiberman, Generally covariant relativistic anisotropic magnetohydrodynamics, *Phys. Rev. E* **51**, 4901 (1995).
- [55] X. G. Huang, A. Sedrakian, and D. H. Rischke, Kubo formulas for relativistic fluids in strong magnetic fields, *Ann. Phys. (N.Y.)* **326**, 3075 (2011).

- [56] B. Giacomazzo and L. Rezzolla, The Exact solution of the Riemann problem in relativistic MHD, *J. Fluid Mech.* **562**, 223 (2006).
- [57] C. Bonati, M. D'Elia, M. Mariti, F. Negro, and F. Sanfilippo, Magnetic Susceptibility of Strongly Interacting Matter across the Deconfinement Transition, *Phys. Rev. Lett.* **111**, 182001 (2013).
- [58] P. Huovinen and P. Petreczky, QCD Equation of State and Hadron Resonance Gas, *Nucl. Phys. A* **837**, 26 (2010).
- [59] C. Shen, U. Heinz, P. Huovinen, and H. Song, Systematic parameter study of hadron spectra and elliptic flow from viscous hydrodynamic simulations of Au+Au collisions at  $\sqrt{s_{NN}} = 200$  GeV, *Phys. Rev. C* **82**, 054904 (2010).
- [60] P. F. Kolb, J. Sollfrank, and U. W. Heinz, Anisotropic flow from AGS to LHC energies, *Phys. Lett. B* **459**, 667 (1999).
- [61] V. Roy and A. K. Chaudhuri, Charged particle's elliptic flow in 2+1D viscous hydrodynamics at LHC ( $\sqrt{s} = 2.76$  TeV) energy in Pb+Pb collision, *Phys. Lett. B* **703**, 313 (2011).
- [62] D. H. Rischke, S. Bernard, and J. A. Maruhn, Relativistic hydrodynamics for heavy ion collisions. I. General aspects and expansion into vacuum, *Nucl. Phys. A* **595**, 346 (1995).
- [63] S. Gupta, The Electrical conductivity and soft photon emissivity of the QCD plasma, *Phys. Lett. B* **597**, 57 (2004).
- [64] M. Greif, I. Bouras, C. Greiner, and Z. Xu, Electric conductivity of the quark-gluon plasma investigated using a perturbative QCD based parton cascade, *Phys. Rev. D* **90**, 094014 (2014).
- [65] S. I. Finazzo and J. Noronha, Holographic calculation of the electric conductivity of the strongly coupled quark-gluon plasma near the deconfinement transition, *Phys. Rev. D* **89**, 106008 (2014).
- [66] J. Błoczyński, X. G. Huang, X. Zhang, and J. Liao, Azimuthally fluctuating magnetic field and its impacts on observables in heavy-ion collisions, *Phys. Lett. B* **718**, 1529 (2013).
- [67] J. Błoczyński, X. G. Huang, X. Zhang, and J. Liao, Charge-dependent azimuthal correlations from AuAu to UU collisions, *Nucl. Phys. A* **939**, 85 (2015).
- [68] W. T. Deng and X. G. Huang, Electric fields and chiral magnetic effect in Cu+Au collisions, *Phys. Lett. B* **742**, 296 (2015).
- [69] W. T. Deng, X. G. Huang, G. L. Ma, and G. Wang, Test the chiral magnetic effect with isobaric collisions, *Phys. Rev. C* **94**, 041901 (2016).